Pergamon

Int. J. Solids Structures Vol. 34, No. 30, pp. 3911–3921, 1997

0020–7683/97 $17.00 + .00

PII: S0020–7683(96)00239–9

ON THE PENNY-SHAPED CRACK IN A NONHOMOGENEOUS INTERLAYER OF ADJOINING TWO DIFFERENT ELASTIC MATERIALS

WANG XUYUE†, ZOU ZHENZHU‡ and WANG DUO†

† Department of Astronautics and Mechanics, Harbin Institute of Technology, Harbin, 150001, People's Republic of China

‡ Department of Transportation, Shijiazhuang Railway Institute, Shijiazhuang, 050043, People's Republic of China

(*Received* 27 *July* 1996; *in revised form* 12 *November* 1996)

Abstract—The torsional problem of a penny-shaped crack at the interface between two distinctly different materials is investigated by presenting the generalized interlayer model. Dislocation density function and integral transform are used to reduce the problem to the singular integral equation. Numerical examples are given to show the effects of the interlayer thickness, distribution parameter, and local nonhomogeneous material property on the stress intensity factor which is obtained by solving a singular integral equation. © 1997 Elsevier Science Ltd.

1. INTRODUCTION

Due to the interpenetration (Williams, 1959) between the interface crack surfaces, modes I and II are coupled and no proper definition for the stress intensity factor is given. To overcome this pathological phenomenon, small scale contact zones (see, e.g., Rice, 1988, Comninou, 1977, Achenbach *et al.* 1979), elastic-plastic analysis (see, e.g., Shih and Asaro 1988, Wang, 1990) and interlayer models (see, e.g., Atkinson, 1977, Ozturk and Erdogan, 1993, 1995, Delale and Erdogan, 1988) are presented. Erdogan has introduced an interlayer model that depends completely on interlayer thickness and material properties. Erdogan's modulus distribution is given as $\mu_2(z) = \mu_1 \exp(z/h \ln \mu_3/\mu_1)$, however, we present a more general interlayer model: $\mu_2(z) = (a+bz)^k$ with distribution parameter k independent of interlayer thickness h and material properties. As the limiting case, Erdogan's modulus distribution can be obtained as $k \to \infty$ with $a = \sqrt[k]{\mu_1}$, $b = (\sqrt[k]{\mu_3} - \sqrt[k]{\mu_1})/h$. The continuity of the elastic modulus leads to the usual square root singularity and avoids the oscillatory behavior. As an example, by virtue of this generalized interlayer model, we treat an interface penny-shaped crack under torsion, and the treatment is based on the use of dislocation density function and integral transform. Numerical results, which are obtained by solving a singular integral equation, indicate the effects of interlayer thickness, local nonhomogeneous elastic property, adjacent material combination and especially the distribution parameter k on the stress intensity factor.

2. BASIC EQUATIONS AND SINGULAR INTEGRAL EQUATION

Consider the penny-shaped crack problem shown in Fig. 1. It is assumed that the applied loads acting in the circumferential direction are axisymmetric. The material-1 and material-3 may be assumed to be unbounded. Thus, the displacement $U_\theta = v$ and the stress components $\sigma_{\theta r}$ and $\sigma_{\theta z}$ are the only nonvanishing quantities. The basic equilibrium equations are as follows:

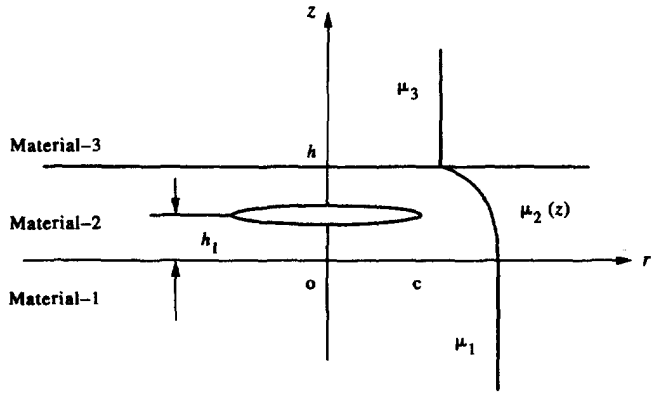

Fig. 1. Interface penny-shaped crack, $\mu_2(z) = (a+bz)^k$, and $\mu_1 = \text{const.}$, $\mu_3 = \text{const.}$, $\mu_2(0) = \mu_1$, $\mu_2(h) = \mu_3$.

$$\frac{\partial \sigma^i_{\theta r}}{\partial r} + \frac{\partial \sigma^i_{\theta z}}{\partial z} + \frac{2}{r}\sigma^i_{\theta r} = 0 \quad i = 1,2,3. \tag{1}$$

Substituting constitutive relations

$$\sigma^i_{\theta z} = \mu_i \frac{\partial v_i}{\partial z}, \quad \sigma^i_{\theta r} = \mu_i\left(\frac{\partial v_i}{\partial r} - \frac{v_i}{r}\right) \quad i = 1,2,3 \tag{2}$$

into (1), we obtain

$$\frac{\partial^2 v_i}{\partial r^2} + \frac{1}{r}\frac{\partial v_i}{\partial r} - \frac{v_i}{r^2} + \frac{\partial^2 v_i}{\partial z^2} = 0 \quad i = 1,3, \tag{3}$$

$$\frac{\partial^2 v_2}{\partial r^2} + \frac{1}{r}\frac{\partial v_2}{\partial r} - \frac{v_2}{r^2} + \frac{\partial^2 v_2}{\partial z^2} + \frac{\mu_2'(z)}{\mu_2(z)}\frac{\partial v_2}{\partial z} = 0, \tag{4}$$

where $i = 1,2,3$ refer to the materials in Fig. 1.

The boundary conditions are as follows:

$$\sigma^1_{\theta z}(r,0) = \sigma^2_{\theta z}(r,0) \quad 0 \leqslant r < +\infty, \tag{5}$$

$$v_1(r,0) = v_2(r,0) \quad 0 \leqslant r < +\infty, \tag{6}$$

$$v_2(r,h_1^-) = v_2(r,h_1^+) \quad r \geqslant c, \tag{7}$$

$$\sigma^2_{\theta z}(r,h_1^-) = \sigma^2_{\theta z}(r,h_1^+) \quad 0 \leqslant r < +\infty, \tag{8}$$

$$\sigma^2_{\theta z}(r,h_1^-) = P_0 = \text{const.} \quad 0 \leqslant r \leqslant c, \tag{9}$$

$$v_2(r,h) = v_3(r,h) \quad 0 \leqslant r < +\infty, \tag{10}$$

$$\sigma^2_{\theta z}(r,h) = \sigma^3_{\theta z}(r,h) \quad 0 \leqslant r < +\infty. \tag{11}$$

Introducing the Hankel transform of the first order, v_i can be expressed as

$$v_i(r,z) = \int_0^\infty V_i(z,\rho)J_1(\rho r)\rho\,\mathrm{d}\rho \quad i = 1,2,3, \tag{12}$$

where $J_1()$ is the Bessel function of the first kind.

From eqns (12), (3), (4), we obtain that

$$\frac{\partial^2 V_i(z,\rho)}{\partial z^2} - \rho^2 V_i(z,\rho) = 0 \quad i = 1,3, \tag{13}$$

$$\frac{\partial^2 V_2(z,\rho)}{\partial z^2} + \frac{\mu_2'(z)}{\mu_2(z)}\frac{\partial V_2(z,\rho)}{\partial z} - \rho^2 V_2(z,\rho) = 0. \tag{14}$$

Considering the regularity condition at $|z| \to \infty$, solutions can be expressed as

$$V_1(z,\rho) = A_1 e^{\rho z} \quad z < 0, \tag{15}$$

$$V_3(z,\rho) = A_4 e^{-\rho z} \quad z > h, \tag{16}$$

and

$$V_2(z,\rho) = A_2(a+bz)^{-\beta} I_\beta\left(\frac{a+bz}{|b|}\rho\right) + A_3(a+bz)^{-\beta} K_\beta\left(\frac{a+bz}{|b|}\rho\right) \quad 0 < z < h_1, \tag{17}$$

$$V_2(z,\rho) = A_2'(a+bz)^{-\beta} I_\beta\left(\frac{a+bz}{|b|}\rho\right) + A_3'(a+bz)^{-\beta} K_\beta\left(\frac{a+bz}{|b|}\rho\right) \quad h_1 < z < h, \tag{18}$$

where $\beta = (k-1)/2$, $I_\beta()$, $K_\beta()$ are modified Bessel functions of the first kind and the second kind.

Defining the dislocation density function as

$$g(r) = \frac{1}{r}\frac{\partial}{\partial r}[rv_2(r,h_1^+) - rv_2(r,h_1^-)]. \tag{19}$$

Substituting eqns (15)–(18) into constitutive relations, and then by using boundary conditions (5), (6), (8), (10), (11) and dislocation density function $g(r)$, after complicated treatment, we obtain

$$\sigma_{\theta z}^2(r,h_1^-) = \mu_2(h_1)\int_0^c K(s,r)g(s)s\,\mathrm{d}s, \tag{20}$$

where

$$K(s,r) = \int_0^{+\infty} D(\rho)\rho J_1(\rho r)J_0(\rho s)\,\mathrm{d}\rho. \tag{21}$$

$D(\rho)$ is given in the Appendix. $K(s,r)$ can be further expressed as

$$K(s,r) = K_n(s,r) + K_s(s,r), \tag{22}$$

$$K_n(s,r) = \int_0^{+\infty} (D(\rho)-\alpha)\rho J_1(\rho r)J_0(\rho s)\,\mathrm{d}\rho, \tag{23}$$

$$K_s(s,r) = \alpha \int_0^{+\infty} \rho J_1(\rho r) J_0(\rho s)\,\mathrm{d}\rho = -\frac{\alpha}{\pi}\left[\frac{1}{s(s-r)} + \frac{-s-r+2rM(s,r)}{s(s^2-r^2)}\right], \tag{24}$$

$$\alpha = \lim_{\rho \to +\infty} D(\rho) = -\frac{1}{2}, \tag{25}$$

where

$$M(s,r) = \begin{cases} \dfrac{s}{r}E\left(\dfrac{s}{r}\right) & s < r, \\ \dfrac{s^2}{r^2}E\left(\dfrac{r}{s}\right) - \dfrac{s^2-r^2}{r^2}K\left(\dfrac{r}{s}\right) & s > r. \end{cases} \tag{26}$$

E and K are complete elliptic integrals of the second and first kind, respectively. Thus, by using eqn (9), eqn (20) is converted to

$$P_0 = \mu_2(h_1)\int_0^c \left[\frac{-\alpha}{\pi}\frac{1}{s-r} + sK_n(s,r) + \frac{\alpha}{\pi}\frac{s+r-2rM(s,r)}{s^2-r^2}\right] g(s)\,\mathrm{d}s \quad 0 < r < c, \tag{27}$$

so we obtain a singular integral equation with the generalized Cauchy kernel. We introduce

$$g(s) = \frac{H(s)}{s^{\delta}(c-s)^{\lambda}} \quad 0 < s < c, \tag{28}$$

using methods developed by Erdogan (1975), we obtain the characteristic equations as

$$ctg(\pi\lambda) = 0, \quad \cos(\pi\delta) = 1. \tag{29}$$

Here the problem under consideration is of axisymmetric torsion, so there exists $v_2(0, z) = 0$. The admissible root of (29) is

$$\lambda = \tfrac{1}{2}, \quad \delta = 0. \tag{30}$$

The single-valued condition can be obtained from the definition of $g(s)$

$$\int_0^c sg(s)\,\mathrm{d}s = 0. \tag{31}$$

3. THE SOLUTION

Equations (27) and (31) can be solved after normalizing the interval by defining

$$s = \frac{1+t}{2}c, \quad r = \frac{1+x}{2}c. \tag{32}$$

Equations (27) and (31) are converted to

$$\int_{-1}^{1}\left[\frac{-\alpha}{\pi}\frac{1}{t-x}+\frac{c}{2}Q(t,x)\right]G(t)\,dt=\frac{P_0}{\mu_2(h_1)}, \tag{33}$$

$$\int_{-1}^{1}(1+t)G(t)\,dt=0, \tag{34}$$

where

$$Q(t,x)=\left[sK_n(s,r)+\frac{\alpha}{\pi}\frac{s+r-2rM(s,r)}{s^2-r^2}\right]_{s=(1+t)/2c,\,r=(1+x)/2c}, \tag{35}$$

$$G(t)=g\left(\frac{1+t}{2}c\right). \tag{36}$$

We use a numerical method developed by Erdogan (1975). $G(t)$ is expressed as

$$G(t)=\frac{F(t)}{\sqrt{1+t}}\frac{1}{\sqrt{1-t}}. \tag{37}$$

Expanding $F(t)$ in forms of Chebyshev polynomials gives

$$F(t)=\sum_{n=0}^{\infty}B_nT_n(t). \tag{38}$$

Using the properties of Chebyshev polynomials as follows:

$$\frac{1}{\pi}\int_{-1}^{1}\frac{T_n(t)\,dt}{(t-x)\sqrt{1-t^2}}=\begin{cases}0 & n=0 \quad -1<x<1,\\ U_{n-1}(x) & n=1,2,\ldots \quad -1<x<1,\\ -\dfrac{|x|}{x\sqrt{x^2-1}}\left[x-\dfrac{|x|\sqrt{x^2-1}}{x}\right]^n & n=0,1,\ldots \quad |x|>1,\end{cases} \tag{39}$$

we obtain

$$\frac{1}{\pi}\int_{-1}^{1}\frac{F(t)\,dt}{(t-x_m)\sqrt{1-t^2}}\approx\sum_{j=1}^{p}B_jU_{j-1}(x_m)=\sum_{j=1}^{p}\sum_{l=1}^{n}\frac{B_jT_j(t_l)}{n(t_l-x_m)}=\sum_{l=1}^{n}\frac{F(t_l)}{n(t_l-x_m)}, \tag{40}$$

where

$$T_n(t_l)=0,\quad t_l=\cos\left(\frac{2l-1}{2n}\pi\right),\quad l=1,\ldots n. \tag{41}$$

$$U_{n-1}(x_m)=0,\quad x_m=\cos\left(\frac{\pi m}{n}\right),\quad m=1,\ldots n-1. \tag{42}$$

Equation (34) can be converted to

$$\frac{1}{\pi}\int_{-1}^{1}\frac{(1+t)F(t)\,dt}{\sqrt{1-t^2}}\approx\sum_{l=1}^{n}\frac{1+t_l}{n}F(t_l)=0. \tag{43}$$

Thus, eqns (33) and (34) become

$$\begin{cases} \sum_{l=1}^{n}\left[\dfrac{-\alpha}{t_l-x_m}+\dfrac{\pi c}{2}Q(t_l,x_m)\right]\dfrac{F(t_l)}{n}=\dfrac{P_0}{\mu_2(h_1)}, \\ \sum_{l=1}^{n}\dfrac{1+t_l}{n}F(t_l)=0. \end{cases} \tag{44}$$

$F(t_l)$ can be obtained by solving this system of linear algebraic equations.

In deriving the singular integral equation, we find that the right-hand side of eqn (27) represents $\sigma^2_{\theta z}(r,h_1)$ within $(0,c)$ as well as outside $(0,c)$, that is to say

$$\sigma^2_{\theta z}(r,h_1)=\mu_2(h_1)\int_0^c\left[\frac{-\alpha}{\pi}\frac{1}{s-r}+sK_n(s,r)+\frac{\alpha}{\pi}\frac{s+r-2rM(s,r)}{s^2-r^2}\right]g(s)\,\mathrm{d}s \quad r>c. \tag{45}$$

Substituting eqn (45) into the definition of stress intensity factor

$$K_3=\lim_{r\to c^+}\sqrt{2(r-c)}\sigma^2_{\theta z}(r,h_1) \tag{46}$$

and using eqns (36)–(39), we obtain

$$K_3=-\frac{1}{2}\mu_2(h_1)\sqrt{\frac{c}{2}}\sum_{n=0}^{\infty}B_n. \tag{47}$$

From eqn (38) it can be obtained that

$$\sum_{n=0}^{\infty}B_nT_n(1)=\sum_{n=0}^{\infty}B_n=F(1), \tag{48}$$

so we obtain

$$K_3=-\frac{1}{2}\mu_2(h_1)\sqrt{\frac{c}{2}}F(1), \tag{49}$$

where $F(1)$ can be obtained by interpolation.

The strain energy release rate

$$\vartheta\,\mathrm{d}c=\int_c^{c+\mathrm{d}c}\frac{1}{2}\sigma^2_{\theta z}(r,h_1)[v_2(r-\mathrm{d}c,h_1^+)-v_2(r-\mathrm{d}c,h_1^-)]\,\mathrm{d}r. \tag{50}$$

Using the asymptotic relations

$$\sigma^2_{\theta z}(r,h_1)\approx\frac{K_3}{\sqrt{2(r-c)}}, \tag{51}$$

$$v_2(r,h_1^+)-v_2(r,h_1^-)\approx\frac{2\sqrt{2(c-r)}}{\mu_2(h_1)}K_3. \tag{52}$$

The above two relations can be asymptotically obtained from eqns (46), (19), (36), (37) and (49), and we can obtain that

$$\vartheta=\frac{\pi}{2}\frac{K_3^2}{\mu_2(h_1)}. \tag{53}$$

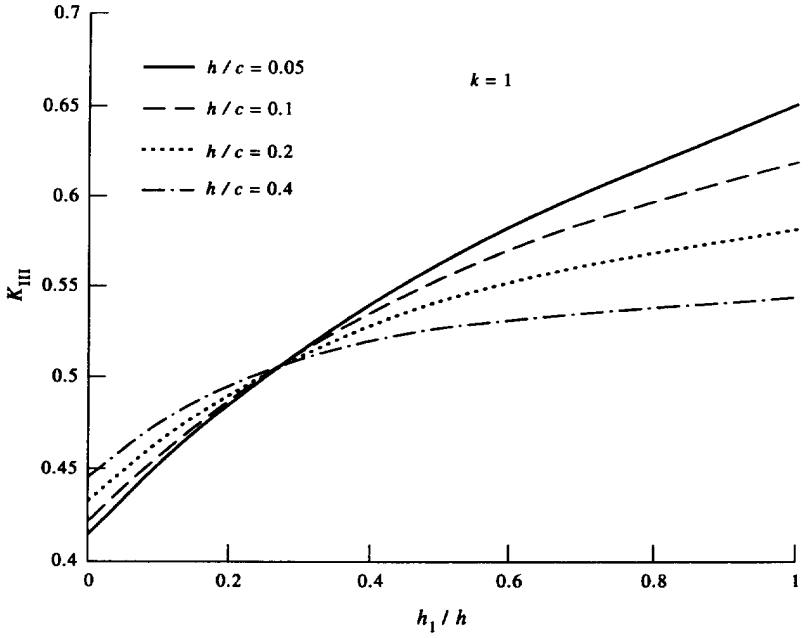

Fig. 2. Effect of the position of the crack on the stress intensity factor for various interlayer thicknesses.

4. RESULTS AND DISCUSSION

The stress intensity factor and strain energy release rate in numerical example are normalized as

$$K_m = K_3/(P_0\sqrt{c}), \quad V = \mu_1 \vartheta/(P_0^2 c). \tag{54}$$

In numerical procedure, for the fixed interlayer thickness h/c and fixed material combination μ_1/μ_3, the number of discrete points n is effected by the crack position h_1/h, as the crack approaches the stiffer medium, the number of n will increase to keep the desired accuracy. However, in our numerical example, $n = 39$ can make sure that the results are accurate within 0.00001 at least.

In Fig. 2, different than the earlier conclusion for a piecewise homogeneous layered medium, which indicates that if the crack approaches a stiffer medium, the stress intensity factor decreases, the results from our nonhomogeneous interlayer model show that the stress intensity factor increases with an increase in the value of h_1/h as $\mu_1 < \mu_3(\mu_1/\mu_3 = 1/3)$. The results in Fig. 2 indicate that, as the value of h_1/h increases, the increase in the stress intensity factor results from the increase in the local elastic modulus, and the local nonhomogeneous elastic modulus $\mu_2(z)$ determines the stress intensity factor rather than the elastic properties of the adjacent materials.

In Fig. 3, the results indicate that, with $\mu_1/\mu_3 = 1/3$, for various interlayer thicknesses, the increase in the local nonhomogeneous elastic modulus results in the decrease in the strain energy release rate, and as the interlayer thickness $h/c \to 0$, the strain energy release rate approaches the constant that represents the strain energy release rate as $h = 0$. It can be seen that the strain energy release rate keeps continuity as interlayer thickness approaches zero.

In Fig. 4, with $h_1/h = 0.5$, $\mu_1/\mu_3 = 1/3$, the results indicate that the stress intensity factor decreases with an increase in the interlayer thickness h/c for various distribution parameters, and on the other hand, it can be seen that, for any fixed interlayer thickness, the stress intensity factor decreases with the increase in the distribution parameter as the crack position is situated at the center of the interlayer.

In Figs 5 and 6, we give the case where $h/c = 0.1$, $\mu_1/\mu_3 = 1/3$. First, we find the dependence of the stress intensity factor and strain energy release rate on the value of h_1/h

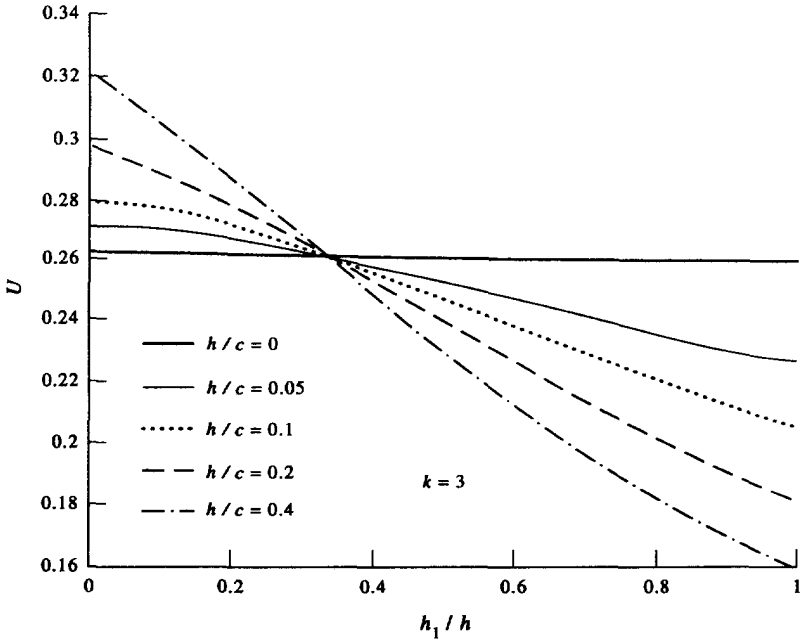

Fig. 3. Effect of the position of the crack on the strain energy release rate for various interlayer thicknesses.

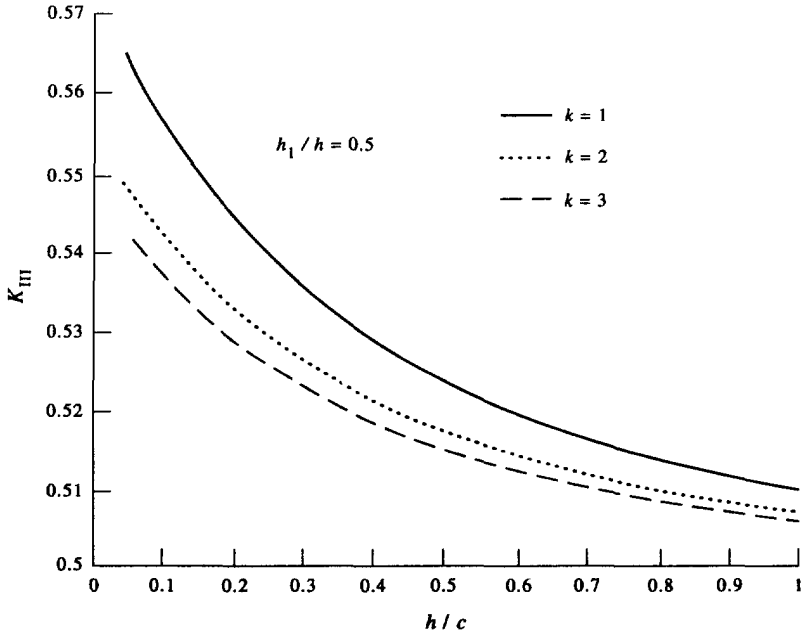

Fig. 4. Effect of the interlayer thickness on the stress intensity factor for various distribution parameters.

as in Fig. 2 and Fig. 3. Secondly, the results indicate that the distribution parameter k inserts remarkable effect on the stress intensity factor, in Fig. 5, with any fixed h_1/h in the domain of about 0–0.037 or 0.9–1, the effect of the distribution parameter on the stress intensity factor is contrary to that with any fixed value of h_1/h in the domain of about 0.037–0.9, and the results in Fig. 6 show that the strain energy release rate increases with an increase in the distribution parameter for any fixed crack position.

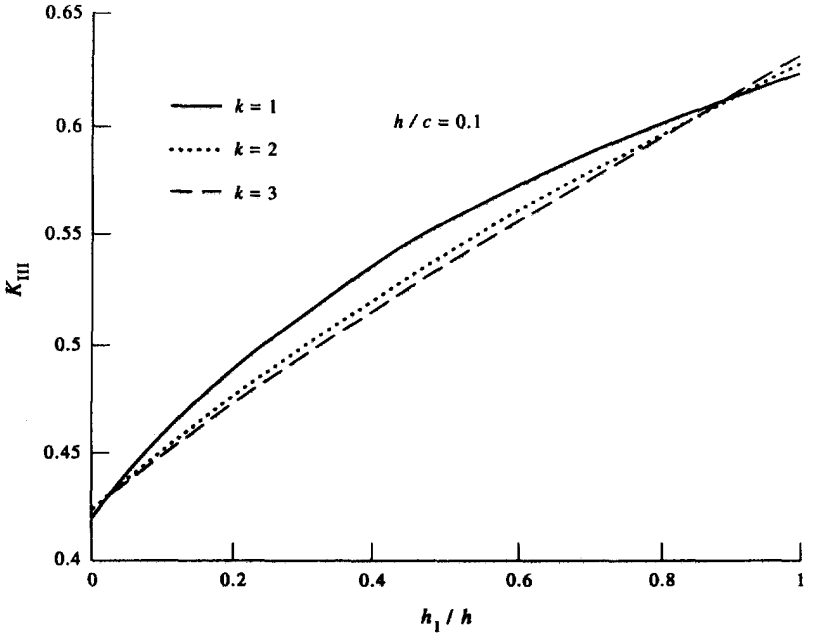

Fig. 5. Effect of the distribution parameter on the stress intensity factor for various crack positions.

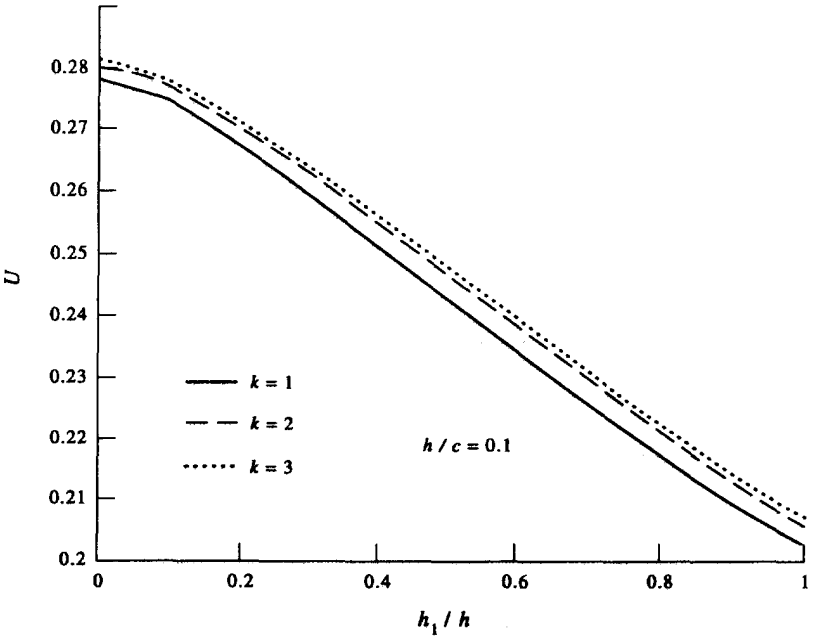

Fig. 6. Effect of the distribution parameter on the strain energy release rate for various crack positions.

In Fig. 7, with $k = 2$, $h/c = 0.1$, the results indicate that, as $h_1/h \geqslant 0.6$, the stress intensity factor steeply decreases with the increase in the value of μ_1/μ_3, and for $h_1/h = 0.2$ or $h_1/h = 0.4$, as the value of μ_1/μ_3 increases, after a dramatic decrease, the stress intensity factor slowly increases, as for the case where $h_1/h = 0$, the stress intensity factor gradually increases with the increase in the value of μ_1/μ_3. Noticing that the difference in the value of μ_1/μ_3 reflects the difference in local nonhomogeneous elastic modulus $\mu_2(z) = (a+bz)^k$ with $a = \sqrt[k]{\mu_1}$, $b = (\sqrt[k]{\mu_3} - \sqrt[k]{\mu_1})/h$, we again see the effect of local nonhomogeneous elastic modulus on the stress intensity factor for any fixed crack position.

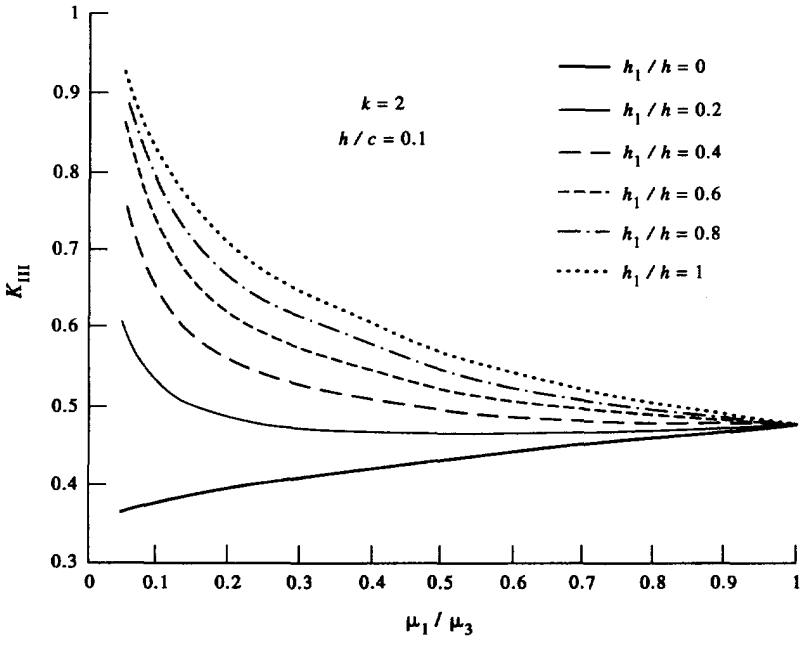

Fig. 7. Effect of the material combination on the stress intensity factor for various crack positions.

REFERENCES

Achenbach, J., Keer, L., Khetan, R. and Chen, S. (1979) Loss of adhesion at the tip of an interface crack. *Journal of Elasticity* **9**, 397–424.

Atkinson, C. (1977) On stress singularities and interfaces in linear elastic fracture mechanics. *International Journal of Fracture* **13**, 807–820.

Comninou, M. (1977) The interface crack. *Journal of Applied Mechanics* **44**, 631–636.

Delale, F. and Erdogan, F. (1988) On the mechanical modeling of the interfacial region in bonded half planes. *Journal of Applied Mechanics* **55**, 317–324.

Erdogan, F. (1975) Complex function technique. In *Continuum Physics*, Vol II, pp. 523–603. Academic Press, New York.

Ozturk, M. and Erdogan, F. (1993) Antiplane shear crack problem in bonded materials with a graded interfacial zone. *International Journal of Engineering Science* **31**, 1641–1657.

Ozturk, M. and Erdogan, F. (1995) An axisymmetric crack in bonded materials with a nonhomogeneous interfacial zone under torsion. *Journal of Applied Mechanics* **62**, 116–125.

Rice, J. (1988) Elastic fracture mechanics concepts for interface cracks. *Journal of Applied Mechanics* **55**, 98–103.

Shih, C. and Asaro, R. (1988) Elastic-plastic analysis of cracks on bimaterials interfaces. Part I: small scale yielding. *Journal of Applied Mechanics* **55**, 299–316.

Wang, T. (1990) Elastic-plastic asymptotic fields for cracks on bimaterial interfaces. *Engineering Fracture Mechanics* **37**, 527–538.

Williams, M. (1959) The stresses around a fault or crack in dissimilar media. *Bulletin of the Seismological Society of America* **49**, 199–204.

APPENDIX

$$D(\rho) = \frac{[L_{61}(L_{22}-\rho L_{12})+L_{62}(\rho L_{11}-L_{21})][L_{61}(\rho L_{32}+L_{42})-L_{62}(\rho L_{31}+L_{41})]}{(L_{51}L_{62}-L_{61}L_{52})[(\rho L_{11}-L_{21})(\rho L_{32}+L_{42})-(\rho L_{31}+L_{41})(\rho L_{12}-L_{22})]}$$

$$L_{11} = a^{-\beta} I_\beta\left(\frac{a}{|b|}\rho\right) \quad L_{12} = a^{-\beta} K_\beta\left(\frac{a}{|b|}\rho\right)$$

$$L_{21} = -ba^{-\beta-1}\beta I_\beta\left(\frac{a}{|b|}\rho\right)+a^{-\beta}\frac{b}{|b|}\rho I_\beta^1\left(\frac{a}{|b|}\rho\right)$$

$$L_{22} = -ba^{-\beta-\nu}\beta K_\beta\left(\frac{a}{|b|}\rho\right)+a^{-\beta}\frac{b}{|b|}\rho K_\beta'\left(\frac{a}{b}\rho\right)$$

$$L_{31} = (a+bh)^{-\beta} I_\beta\left(\frac{a+bh}{|b|}\rho\right) \quad L_{32} = (a+bh)^{-\beta} K_\beta\left(\frac{a+bh}{|b|}\rho\right)$$

$$L_{41} = -b\beta(a+bh)^{-\beta-1}I_\beta\left(\frac{a+bh}{|b|}\rho\right)+(a+bh)^{-\beta}\frac{b}{|b|}\rho I'_\beta\left(\frac{a+bh}{|b|}\rho\right)$$

$$L_{42} = -b\beta(a+bh)^{-\beta-1}K_\beta\left(\frac{a+bh}{|b|}\rho\right)+(a+bh)^{-\beta}\frac{b}{|b|}\rho K'_\beta\left(\frac{a+bh}{|b|}\rho\right)$$

$$L_{51} = \rho(a+bh_1)^{-\beta}I_\beta\left(\frac{a+bh_1}{|b|}\rho\right) \quad L_{52} = \rho(a+bh_1)^{-\beta}K_\beta\left(\frac{a+bh_1}{|b|}\rho\right)$$

$$L_{61} = -b\beta(a+bh_1)^{-\beta-1}I_\beta\left(\frac{a+bh_1}{|b|}\rho\right)+(a+bh_1)^{-\beta}\frac{b\rho}{|b|}I'_\beta\left(\frac{a+bh_1}{|b|}\rho\right)$$

$$L_{62} = -b\beta(a+bh_1)^{-\beta-1}K_\beta\left(\frac{a+bh_1}{|b|}\rho\right)+(a+bh_1)^{-\beta}\frac{b\rho}{|b|}K'_\beta\left(\frac{a+bh_1}{|b|}\rho\right).$$